5.13 A DIAGNOSTIC STUDY OF EPISODIC MIXING MODELS OF SHALLOW CUMULUS CLOUDS

Ming Zhao* and Philip H. Austin
University of British Columbia, Vancouver, Canada

1. Introduction

Shallow cumulus clouds play a fundamental role in the vertical redistribution of energy and moisture in the lower troposphere. While their influence is well established, there are currently a wide range of approaches to represent the ensemble effect of these clouds in large-scale models. This breadth of approach is understandable given lack of consensus as to the mechanism by which turbulent clouds mix with their surroundings [see, e.g. Blyth, 1993; Siebesma, 1998; Emanuel, 1994].

Episodic mixing and buoyancy sorting (EMBS) models are motivated by observations of cloud structure that suggest undilute subcloud air (USCA) is present at well above cloud base. Episodic mixing idealizes a cloud as a core updraft of (USCA), part of which mixes with environmental air at each vertical level. The mixing is envisioned as occurring in eddies that create a spectrum of mixtures ranging from pure subcloud air to pure ambient air. Buoyancy-sorting assumes that the generated individual mixtures are primarily driven by their own buoyancy against the environment and are eventually detrained from their individual neutral buoyancy level (NBL). While EMBS models can make a claim for a physically more realistic representation of cloud mixing, they obviously represent a highly idealized picture of cloud environment mixing, and require the specification of three pieces of information for which there are few observational constraints: 1) the rate at which USCA is shed by the undiluted thermal (which we will refer to as the undilute eroding rate, or UER); 2) the mass distribution of cloud mixtures following a mixing event; and 3) a detrainment criterion to specify the vertical level of detrained cloud parcels.

In this study we investigate the capability of the EMBS model in representation of nonprecipitating cumulus clouds. In particular, we retrieve the UER, which constitutes a major assumption in all EMBS models [Emanuel and Zivkovic-Rothman, 1999] (EZ99) based on the observed large-scale forcing and equilibrium state of a trade cumulus atmosphere, given a fixed mixtures mass distribution and a detrainment criterion. In Section 2 we introduce the EMBS model and the diagnostic approach. In Section 3, we present a case study and its results. In Section 4 we discuss the results and its implication to the parameterization of cumulus ensemble.

*Corresponding author address: Ming Zhao, Atmospheric Science Programme, Earth and Ocean Sciences Department, University of British Columbia, Vancouver, B.C., V6T 1Z2, Canada; email: mzhao@eos.ubc.ca

2. Approach

2.1. Mass flux parameterization

For an environment containing non-precipitating cumuli with small cloud-fraction, the conservation equations for environmental entropy and total water, averaged over a region containing many clouds, can be written as [e.g Arakawa and Schubert, 1974; Emanuel, 1994]

$$\frac{\partial \theta_l}{\partial t} + V_H \nabla \theta_l - \rho g w \frac{\partial \theta_l}{\partial p} + Q_R = \underbrace{-g M_f \frac{\partial \theta_l}{\partial p}}_{I} + \underbrace{g(\theta_{l,c} - \theta_l) D}_{II} \quad \text{(1a)}$$

$$\frac{\partial q_t}{\partial t} + V_H \nabla q_t - \rho g w \frac{\partial q_t}{\partial p} = \underbrace{-g M_f \frac{\partial q_t}{\partial p}}_{I} + \underbrace{g(q_{t,c} - q_t) D}_{II} \quad \text{(1b)}$$

where θ_l is liquid water potential temperature and q_t is total water specific humidity. The RHS terms are tendencies due to cumulus sub-grid scale transport. Term I represents the effect of cloud-induced environmental compensating vertical motion. M_f is the averaged vertical cloud mass flux. Term II represents lateral detrainment of the temperature and moisture difference between cloudy air and the environment air. In a large-scale model, EMBS models parameterize and provide values for M_f and the cloud detrainment. Alternatively, if we know the large scale forcing from an observational study of equilibrium convection, we may diagnose cloud thermodynamic properties and some critical model parameters required for equilibrium, based on a specified mixing model.

2.2. EMBS representation – diagnosing $U(i)$

Let i represents any model level between cloud base (ICB) and cloud top (INB). $F(i+1/2)$ represents the mass flux of USCA at any interface level $i+1/2$, $U(i)$ is the change of undilute mass flux F over the depth of level i, $U(i) = F(i-1/2) - F(i+1/2)$. $E(i)$ represents the eroding rate of the USCA at level i, which is defined as the vertical gradient of undilute mass flux, $E(i) = dF/dz \approx U(i)/\Delta z$. We will use "UER" below to refer to both $E(i)$ and the discretized $U(i)$. F_b, the undilute cloud base mass flux, is given by $F_b = \sum_{ICB}^{INB} U(i)$. At each level i, N mixtures are generated and given a unique label j. The fraction of environment air in the jth mixture generated at level i is denoted by $\sigma^{i,j}$, while $P(\sigma^{i,j})$ is the normalized USCA mass distribution in the generated spectrum of mixtures. Therefore, the mass component of USCA in each of the mixtures is $u^{i,j} = P(\sigma^{i,j})U(i)$, and the total mass of each of the mixtures is $m^{i,j} = u^{i,j}/(1-\sigma^{i,j})$.

Assuming mixing is strictly linear in the conserved vari-

ables θ_l and q_t, we have

$$\theta_l^{i,j} = \sigma^{i,j}\theta_l^i + (1-\sigma^{i,j})\theta_l^u \quad (2a)$$

$$q_t^{i,j} = \sigma^{i,j}q_t^i + (1-\sigma^{i,j})q_t^u \quad (2b)$$

Given the two conserved variables and a pressure level, we can calculate all other thermodynamic variables of the mixture, which include virtual potential temperature $\theta_v^{i,j}$ (including the liquid water loading effect) and the liquid water virtual potential temperature $\theta_{lv}^{i,j}$. These two variables may be utilized to determine which level a mixture should leave the clouds in an EMBS model – the collection of all mixtures detraining at a particular level gives the detraining cloud mixtures $\theta_{l,c}$ and $q_{t,c}$ in (1). We will adopt the approach of Emanuel [1991] and assume mixtures detrain at their unsaturated neutral buoyancy level (UNBL), defined as levels where the parcel and environment have equal θ_{lv}. This detrainment criterion simulates multiple mixing events which follow detrainment, with evaporation of all liquid water and cooling of the mixture. Detrainment at the UNBL corresponds to a cloud-environment boundary such that the cloud envelope includes a moist near-cloud region which is free of liquid water but part of the cloud-induced convective circulation

Given the detrainment criterion, we can collect all the mixtures mixing at level n and detraining at level k. A discretized version of (1) may then be written as

$$-g\left(\frac{\partial\theta_l}{\partial p}\right)^i \sum_{n=i}^{INB}\left[U(n)+\sum_{k=1}^{i-1}(MENT^{k,n}-MENT^{n,k})\right] + \frac{g}{\Delta p}\sum_{n=ICB}^{INB} TENT^{n,i} = F_t^i \quad (3a)$$

$$-g\left(\frac{\partial q_t}{\partial p}\right)^i \sum_{n=i}^{INB}\left[U(n)+\sum_{k=1}^{i-1}(MENT^{k,n}-MENT^{n,k})\right] + \frac{g}{\Delta p}\sum_{n=ICB}^{INB} QENT^{n,i} = F_q^i \quad (3b)$$

where F_t^i and F_q^i represent the sum of all large-scale forcings of θ_l and q_t respectively. $MENT^{n,k}$ represent the total mass of mixtures generated at level n and detrained at level k. $QENT^{n,i}$ and $TENT^{n,i}$ represent the total mass weighted excess of q_t and θ_l for all mixtures generated at level n and detrained at level i.

$$MENT^{n,k} = \sum_j^{\theta_{lv}^{n,j}=\theta_{lv}^k} \frac{P(\sigma^{n,j})}{1-\sigma^{n,j}}U(n) = A^{n,k}U(n) \quad (4)$$

$$QENT^{n,i} = \sum_j^{\theta_{lv}^{n,j}=\theta_{lv}^i} \frac{P(\sigma^{n,j})}{1-\sigma^{n,j}}U(n)(q_t^{n,j}-q_t^i) = B^{n,i}U(n) \quad (5)$$

$$TENT^{n,i} = \sum_j^{\theta_{lv}^{n,j}=\theta_{lv}^i} \frac{P(\sigma^{n,j})}{1-\sigma^{n,j}}U(n)(\theta_l^{n,j}-\theta_l^i) = C^{n,i}U(n) \quad (6)$$

Inserting (4, 5 and 6) into (3), we find two sets of linear equations for $U(i)$. If large-scale forcings, the mass distribution of generated mixtures and a detrainment criterion are given, (3a) and (3b) may be solved independently. As a consistency check, we can, for example, find $U(i)$ based on (3a) and substitute it into the (3b) to confirm that it produces an equilibrium profile for q_t, given the tight coupling of θ_l and q_t via mixing and detrainment.

Below we follow Emanuel [1991] and assume a mixing distribution $P(\sigma^{i,j})$=$1/N$, i.e. at each of the model level $U(i)$ is split equally, then mixes with different proportions of environment air.

3. Case study and results

We choose the undisturbed trade wind cumulus clouds from BOMEX Phase III case to investigate the EMBS model considering its well-observed equilibrium state. The actual soundings and large-scale forcings used here are from the Large Eddy Simulation (LES) generated equilibrium state (the 5-6th hour averaged mean profiles from the KNMI model) and its specified large-scale forcings. For a detailed description of the experiment, please refer Siebesma et al. [2002].

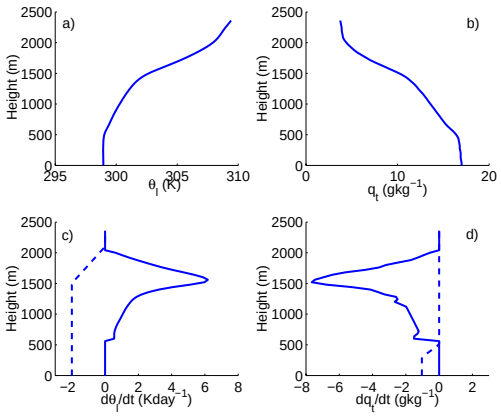

Figure 1. BOMEX equilibrium state. a) θ_l. b) q_t. c) solid line: θ_l subsidence tendency $-\rho g w\frac{\partial\theta_l}{\partial p}$; dashed line: radiative cooling Q_R; d) solid line: q_t tendency due to subsidence $-\rho g w\frac{\partial q_t}{\partial p}$, dashed line: large scale advective drying $V_H\nabla q_t$

Fig. 1 a) and b) are horizontally averaged vertical profiles of the LES output for θ_l and q_t. It shows the typical layer structure for the trade cumulus boundary layer: a well-mixed sub-cloud layer between approximately 0 - 500 m, a conditionally unstable cloud layer between 500 - 1500 m, and an overlying inversion layer. Fig. 1 c) and d) are the calculated large-scale forcings of θ_l and q_t based on the LES specified large-scale subsidence, radiative cooling and subcloud layer advective drying. Since the averaged atmospheric state maintains an approximate equilibrium during the simulation period and also during

the several days of the field experiment, we expect that the cumulus cloud response balances the net large-scale forcing in the cloud layer and inversion layer. Therefore Fig. 1 indicates the cumulus ensemble cools and moistens the inversion layer and heats and moistens the cloud layer.

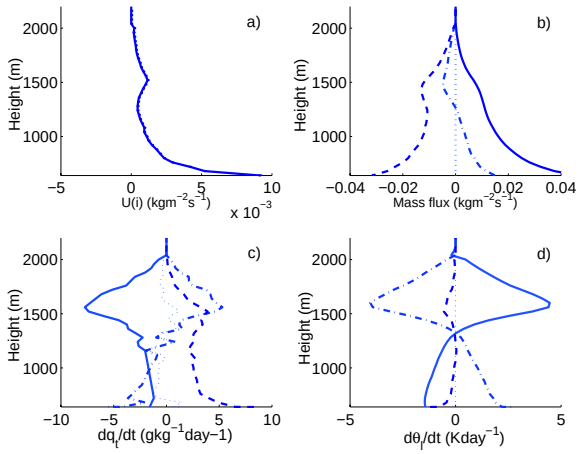

Figure 2. Diagnosed results based on the EMBS model. $U(i)$ is obtained by solving (3a). a) the retrieved $U(i)$; b) solid line: mass flux from ascending USCA; dashed line: mass flux from descending mixtures; dot-dash line: the total mass flux. c) solid line: large-scale forcing of q_t; dot-dashed line: q_t tendency due to cloud induced vertical mass flux; dashed line: cloud lateral detrained tendency; dotted line: the total net tendency. d): as in c) but for θ_l.

Fig. 2 shows the diagnosed results. Fig. 2 a) gives the UER retrieved by solving (3a). Within the cloud layer, we see the UER decreases exponentially with increasing height. Near the bottom of the inversion, it increases before decreasing almost linearly throughout the inversion layer. Using the diagnosed UER, the model produces a cumulus-induced θ_l tendency which exactly balances the large-scale θ_l tendency. As a consistency check Fig. 2c shows the model-produced q_t tendency balances the large-scale q_t tendency to within the accuracy of the observations.

Fig. 2b shows the diagnosed cloud net mass flux is significantly different from the LES results. The figure shows: 1) The net cloud mass flux within the inversion layer is downward while below the inversion it is upward. The vertical integral of the cloud mass flux induced θ_v tendency is close to zero indicating that non-precipitating clouds only transport θ_v and do not act as net sources or sinks of θ_v. 2) The overall magnitude of upward mass flux within the cloud layer is much smaller than those obtained from the LES. This disparity is due to the different definition of the cumulus cloud boundary, which is linked to the model's detrainment criterion. In the LES, the clouds are defined as saturated cloudy parcels which have liquid water, while the clouds in the EMBS are defined as a convective envelope which can be a short distance away from the actual visible clouds, incorporating cloud evaporation and the associated unsaturated convective downdrafts into the net mass flux. Indeed, in Fig. 2d, we see little lateral detrained θ_l tendency while the detrained water vapor is still significant (Fig. 2c).

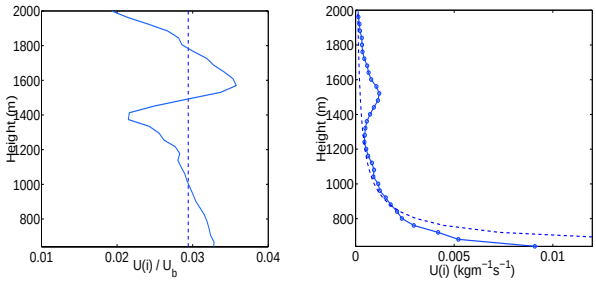

Figure 3. a) Normalized UER for BOMEX cumuli based on RB86 (dashed line) and EZ99 (solid line). b) solid: diagnosed UER replotted from Fig. 2a, dashed: cumulus cloud size/height distribution

Figure 3a,b contrasts the retrieved UER (Fig. 3b) with UER profiles suggested by single-cloud modeling studies [e.g. Bretherton and Smolarkiewicz, 1989] and used by Raymond and Blyth [1986] (RB86) and EZ99 RB86 assumes a constant UER, which means the undilute cloud base mass flux is equally distributed into each model level. EZ99 suggests a formulation (equation (1) in their paper) that assumes entrainment and detrainment rates are functions of the parcel's vertical buoyancy gradient. (calculated here using the equilibrium profiles of Fig. 1)

Figure 3b compares the retrieved UER with a shallow cumulus cloud size distribution calculated from LES results by Neggers et al. [2002]. This size/height distribution is given by

$$N(h) = a(h - h_b)^b \tag{7}$$

where, $b = -1.7$, h_b is cloud-base height (600m for BOMEX), h is cloud-top height, $h - h_b$ is cloud depth or cloud size, Here, a is chosen as 25 in order to scale the cloud number density to the quantities of the UER. We have transformed (7) from cloud horizontal size to cloud height since non-precipitating trade cumuli, on average, are as tall vertically as they are wide horizontally [e.g Betts, 1973].

Fig. 3(b) shows a qualitative match between the retrieved UER and the normalized cloud height/size distribution for small to medium size clouds. Both profiles first rapidly decay near cloud base and then steadily decrease with increasing cloud height/size. In the vicinity of the inversion the sudden change in stability produces increased erosion of USCA. In the next section we discuss links between the UER, the cloud size distribution and the dynamic and thermodynamic response of the cumulus ensemble to large-scale forcing.

4. Discussion

We have tested the sensitivity of the retrieved UER to a range of mixing distributions (see Zhao and Austin [2002] for a complete discussion). The power law decay of the UER seen in Figure 3b is present in all cases that are able to fit large-scale tendencies.

The UER is presumably the cumulative product of a large number clouds, with a broad size distribution. To isolate the mixing effects of individual clouds, we have applied the EMBS with a constant UER to four individual non-precipitating cumuli with cloud-top heights at 2000m, 1500m, 1000m and 800m (and a 600 m cloud base). These cases represent large, middle, small and very small clouds respectively. We find with exception of the smallest cloud that the individual clouds warm and dry their environment near their base while cooling and moistening their environment near their upper part. While these counteracting cloud top and cloud base effects are roughly symmetric for larger clouds, the 200 m thick cloud exhibits moistening and cooling throughout its depth.

In contrast to these individual responses, the cloud ensemble must respond to the BOMEX large-scale forcing by moistening throughout the cloud layer, with a maximum at upper levels, while cooling the upper environment and slightly warming the lower environment (see Fig 1). The disparity between the individual and cumulative effect can be explained through cloud size distribution. To achieve the ensemble cloud response the cloud population has to be organized in such a way so that the cloud-top-moistening of smaller clouds exceeds the larger clouds' cloud-base-drying. Although individually the bigger clouds have a larger convective impact, the large number of smaller clouds more than compensates for this cloud base drying.

The smallest clouds are little more than tracers of subcloud thermals and do not vent subcloud air into upper levels. Nevertheless, by mixing, evaporating, downward transport and detrainment, they contribute significantly to the cloud base water and heat balance by reducing the cloud base heating and drying of deeper, larger and more active clouds. Accurate representation of this cloud base process is crucial to the prediction of cloud base temperature and humidity and the cloud base mass flux. In this sense, accurate representation of the very small clouds is important for large-scale parameterizations.

A consistent picture of the cumulus response to large scale forcing can be constructed as follows. During the adjustment toward the equilibrium state, smaller clouds precondition the environment by continuously cooling and moistening their upper environment. In this way, future ascending subcloud air is subject to less evaporation and becomes more buoyant and as a result, is able to reach higher levels. An equilibrium picture of the cloud ensemble includes the effect of the smallest forced clouds, which feed only from subcloud layer thermals and are suppressed by all larger clouds. In turn slightly larger clouds are supported both from subcloud layer thermals and the smallest clouds, which themselves also feed from subcloud layer thermals. In this way, the largest clouds feed from subcloud layer not only directly from the associated penetrative ascending thermals, but also indirectly from all smaller clouds. It is through this cooperative behavior that the entire population of clouds transports energy and water vapor out of the subcloud layer and redistributes them in the cloud layer.

The preceding analysis emphasizes the importance of including the effect of the cloud population in an episodic mixing cumulus parameterization scheme. In Arakawa and Schubert [1974]'s spectral representation of cumulus clouds, the cloud base mass flux associated with an individual cloud type is determined by the assumption of a quasi-equilibrium energy state (the cloud work function). In transient cumulus cloud models, such as Fraedrich [1976] empirical cloud population statistics are used directly to determine the accumulated mass flux. Similarly, taking account of the cloud population may improve the ability of episodic mixing models to parameterize cumulus convection.

Acknowledgments The authors gratefully acknowledge support from the Natural Science and Engineering Research Council of Canada, the Canadian Foundation for Climate and Atmospheric Science, and the Meteorological Service of Canada.

References

Arakawa, A. and W. H. Schubert, 1974: Interaction of a cumulus cloud ensemble with the large-scale environment, part i. *J. Atmos. Sci.*, **31**, 674–701.

Betts, A. K., 1973: A relationship between stratification, cloud depth, and permitted cloud radii. *J. Appl. Met.*, **12**, 890–893.

Blyth, A. M., 1993: Entrainment in cumulus clouds. *J. Appl. Met.*, **32**, 626–641.

Bretherton, C. S. and P. K. Smolarkiewicz, 1989: Gravity waves, compensating subsidence and detrainment around cumulus clouds. *Journal of the Atmospheric Sciences*, **46**(6), 740–759.

Emanuel, K. A., 1991: A scheme for representing cumulus convection in large-scale models. *J. Atmos. Sci.*, **48**, 2313–2335.

Emanuel, K. A., 1994: *Atmospheric Convection*. Oxford. 580 pp.

Emanuel, K. A. and M. Zivkovic-Rothman, 1999: Development and evaluation of a convection scheme for use in climate models. *J. Atmos. Sci.*, **56**, 1766–1782 (EZ99).

Fraedrich, K., 1976: A mass budget of an ensemble of transient cumulus clouds determined from direct cloud observations. *J. Atmos. Sci.*, **33**, 262–268.

Neggers, K., H. Jonker and A. Siebesma, 2002: Statistics of cumulus cloud populations in large-eddy simulations. *submitted to J. Atmos. Sci*, **.**

Raymond, D. J. and A. M. Blyth, 1986: A stochastic mixing model for nonprecipitating cumulus clouds. *J. Atmos. Sci.*, **43**, 2708–2718 (RB86).

Siebesma, A. P., 1998: Shallow cumlulus convection. in E. J. Plate, E. E. Fedorovich, D. X. Viegas and J. C. Wyngaard, editors, *Buoyant Convection in Geophysical Flows*, pp. 441–486. Kluwer Academic Publishers.

Siebesma, A. P., C. S. Bretherton, A. R. Brown, A. Chlond and et al., 2002: An intercomparison study for cloud resolving models of shallow cumulus convection. *J. Atmos. Sci.*, tbd, in press.

Zhao, M. and P. H. Austin, 2002: A diagnostic study of episodic mixing models of shallow cumulus convection. `http://www.eos.ubc.ca/research/clouds/bl513`.